BNL-226363-2024-TECH

EIC-ADD-TN-112

Crabbing Angle Measurement

I. Pinayev

November 2024

Electron-Ion Collider Project

Brookhaven National Laboratory

U.S. Department of Energy

USDOE Office of Science (SC), Nuclear Physics (NP)

Notice: This technical note has been authored by employees of Brookhaven Science Associates, LLC under Contract No.DE-SC0012704 with the U.S. Department of Energy. The publisher by accepting the technical note for publication acknowledges that the United States Government retains a non-exclusive, paid-up, irrevocable, world-wide license to publish or reproduce the published form of this technical note, or allow others to do so, for United States Government purposes.

DISCLAIMER

This report was prepared as an account of work sponsored by an agency of the United States Government. Neither the United States Government nor any agency thereof, nor any of their employees, nor any of their contractors, subcontractors, or their employees, makes any warranty, express or implied, or assumes any legal liability or responsibility for the accuracy, completeness, or any third party's use or the results of such use of any information, apparatus, product, or process disclosed, or represents that its use would not infringe privately owned rights. Reference herein to any specific commercial product, process, or service by trade name, trademark, manufacturer, or otherwise, does not necessarily constitute or imply its endorsement, recommendation, or favoring by the United States Government or any agency thereof or its contractors or subcontractors. The views and opinions of authors expressed herein do not necessarily state or reflect those of the United States Government or any agency thereof.

Crabbing Angle Measurement

I. Pinayev

Electron-ion collider will employ transverse deflecting (crabbing) cavities to increase luminosity. There will be multiple cavities which will create localized crab bump in the interaction region [1]. For proper compensation of the crossing angle each crab cavity should individually calibrated and phased.

At KEK the crabbing angle was measured with the beam displacement [2] depending on the crab-cavity phase and it is shown in Fig. 1.

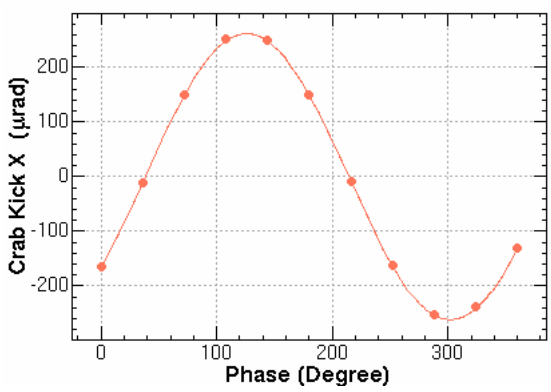


Figure 1: Dependence of the horizontal kick by the crab cavity of the rf phase.

There is a good agreement between the measured kick angle and the estimate from the orbit response. The difference is only 3.6% and might be due to the error in the values of beam functions.

References [3,4] describe usage of streak-camera used to observe the correlation of the beam tilt with the longitudinal position. The proposed method has substantial errors due to the noisy signal from the streak-camera and requires good optical resolution (see Fig. 2).

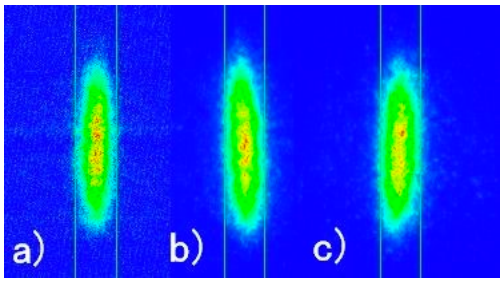


Figure 2: Measurement of the beam tilt with streak-camera. (a) Crab cavity voltage is 0. (b) Crab cavity is ON and a phase of the crab voltage is 0 degree. (c) Crab cavity voltage is ON and the crab phase is 180 degree.

Using beam position monitors (BPMs) allows easily finding the zero-crossing phase of the crab-cavity while the angle requires knowledge of β-functions and phase advances. It also limits the cavity voltage due to possible beam losses on the apertures. For model-independent measurements, we can place two correctors on both sides of the crab cavities and compensate for the orbit distortion caused by a cavity. The BPMs are used as zero indicators, showing that the orbit bump is localized in the crab cavities region. The deflecting angle is the sum of two trim kicks, which can be found from the magnetic measurements and beam rigidity. For a single short cavity there is a possibility to utilize single trim placed next to it, but this will create small step in the orbit.

During regular operations the scanning of the crab cavities is not possible, and streak-camera cannot be used for the hadron beam. In [5-8] it was proposed to measure the longitudinal tilt using phase information from BPM signals. Following the calculations in [8] we can find the phase shift between two electrodes. Charged induced by relativistic beam with gaussian profile on the buttons A (top) and B (bottom) can be described by formulas [9]:

$$\begin{aligned} Q_A(t) &= \frac{qQ_{bunch}}{\sqrt{2\pi}c\sigma}\left(1 + S(y + \alpha ct)\right)exp\left(-\frac{t^2}{2\sigma^2}\right) \\ Q_B(t) &= \frac{qQ_{bunch}}{\sqrt{2\pi}c\sigma}\left(1 - S(y + \alpha ct)\right)exp\left(-\frac{t^2}{2\sigma^2}\right) \end{aligned} \quad (1)$$

where Q_{bunch} (C) is bunch charge, q (m) characterizes pick-up geometry (like the ratio of button surface to pipe diameter), σ (s) is bunch length, S (m^{-1}) is a BPM scaling factor, y (m) is the position of the bunch center (deflection is in the vertical plane), α (radian) is a crabbing angle, c (m/s) is the speed of light. Here we assume that the induced charge is proportional to the bunch linear charge density ($\frac{r}{\gamma c} \ll \sigma$, where r is vacuum chamber radius and γ is a relativistic factor).

The varying button charge will induce a voltage on the cable with impedance Z (neglecting button capacitance):

$$\begin{aligned} U_A(t) &= \frac{ZqQ_{bunch}}{\sqrt{2\pi}c\sigma}\left[S\alpha c\left(1 - \frac{t^2}{\sigma^2}\right) - (1 + Sy)\frac{t}{\sigma^2}\right]exp\left(-\frac{t^2}{2\sigma^2}\right) \\ U_B(t) &= \frac{ZqQ_{bunch}}{\sqrt{2\pi}c\sigma}\left[-S\alpha c\left(1 - \frac{t^2}{\sigma^2}\right) - (1 - Sy)\frac{t}{\sigma^2}\right]exp\left(-\frac{t^2}{2\sigma^2}\right) \end{aligned} \quad (2)$$

The cosine and sine components can be found by using the Fourier transform at a single frequency. The repetition period is T, and the observation is done at angular frequency $\omega = \frac{2\pi h}{T}$, where h is the harmonic number.

$$\begin{aligned} U_{cosA,B} &= \frac{2}{T}\int_{-T/2}^{T/2} U_{A,B}(t)\cos\omega t\, dt \\ U_{sinA,B} &= \frac{2}{T}\int_{-T/2}^{T/2} U_{A,B}(t)\sin\omega t\, dt \end{aligned} \quad (3)$$

For the short bunches ($\sigma \ll T$) the integral limits can be extended to infinity

$$U_{cosA,B} \approx \pm\frac{2}{T}\frac{ZqQ_{bunch}}{\sqrt{2\pi}c\sigma} S\alpha c \int_{-\infty}^{\infty}\left(1-\frac{t^2}{\sigma^2}\right) exp\left(-\frac{t^2}{2\sigma^2}\right)\cos\omega t\, dt$$
$$U_{sinA,B} \approx -\frac{2}{T}\frac{ZqQ_{bunch}}{\sqrt{2\pi}c\sigma^2}(1 \pm Sy)\int_{-\infty}^{\infty}\frac{t}{\sigma} exp\left(-\frac{t^2}{2\sigma^2}\right)\sin\omega t\, dt \quad (4)$$

or

$$U_{cosA,B} \approx \pm\frac{2}{T} ZqQ_{bunch} S\alpha\sigma^2\omega^2 e^{-\frac{\omega^2\sigma^2}{2}}$$
$$U_{sinA,B} \approx -\frac{2}{T}\frac{ZqQ_{bunch}}{c}(1 \pm Sy)\omega e^{-\frac{\omega^2\sigma^2}{2}} \quad (5)$$

For the estimates, we assume that beam displacement is small ($Sy \ll 1$). Then the phases of the signals will be

$$\varphi_{A,B} = \pm\cot^{-1} cS\alpha\sigma^2\omega \quad (6)$$

For small crabbing angles

$$\varphi_B - \varphi_A = 2S\alpha c\sigma^2\omega_{BPM} \quad (7)$$

Experimental measurement of the longitudinal beam tilt in [8] showed factor two difference between theoretical and observed values of the phase shift. Such large discrepancy required additional investigation to find a source of error. This is also essential since the vertical tilt was developed using fast kicker installed in the region with non-zero dispersion [10].

There are two transverse deflecting cavities available at the C-AD complex for the test of the derived equations. The first one is installed in the Coherent electron Cooling (CeC) experiment and the second cavity is used by Low-energy RHIC electron Cooling (LEReC). Both cavities are intended for measurement of the longitudinal profile. We can monitor beam size (current profile and bunch length) for both setups during measurements. The longitudinal tilt can be estimated from the vertical r.m.s. beam size (assuming that the emittance contribution is small) and r.m.s. bunch length. Or it can be calculated from deflecting cavity parameters (U_{cav} and ω_{cav}), beam rigidity *pc* and distance *L* from the cavity to the BPM

$$\alpha = \frac{U_{cav}}{pc}\frac{L\omega_{cav}}{c} \quad (8)$$

Or after the substitution into the Eq. 7

$$\varphi_B - \varphi_A = 2SL\frac{U_{cav}}{pc}\sigma^2\omega_{cav}\omega_{BPM} \quad (9)$$

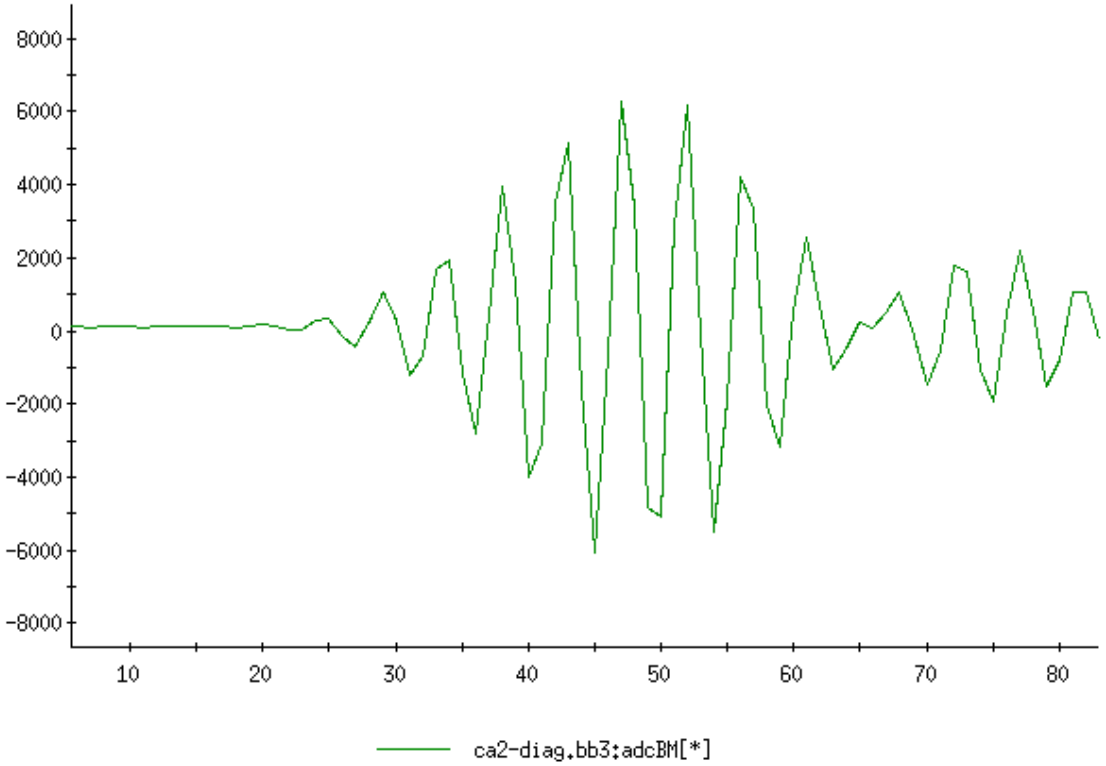


Figure 3: The raw ADC signal from channel B of BPM3 of CeC diagnostics line.

Both systems have Libera Single Bunch BPM [11] with a bandpass filter ringing on the known frequency. The raw ADC data are available for analysis and sample of data is shown in Fig. 3. The ADC sampling rate and hence phase advance per tick are also known. Only the central part of the waveform was used for fit, described by the formula below, and the phase φ in the fit was used for the measurements

$$U(t) = A(1 + at + bt^2)\sin\omega t + \varphi \qquad (10)$$

For LEReC the electron beam energy is E_{kin} = 1.58 MeV (γ=4.1, pc=2.03 MeV). 704 MHz deflecting cavity has 50 kV max voltage. BPM is tuned to 704 MHz ($\omega = 4.42 \times 10^9$) and has scaling factor S=53 m^{-1} (k=19 mm). Distance from the cavity to BPM is 0.43 m, and to the screen is 1.96 m.

The longitudinal profile of the LeREC bunch current is shown in Fig. 4. The profile is close to the gaussian shape with r.m.s. bunch bunch length of 32.7 ps. Using Eq. 8 and 9 we can estimate that bunch longitudinal tilt at the location of BPM will be 124.8 mrad for 40 kV cavity voltage, and corresponding phase shift is 18.8 mrad.

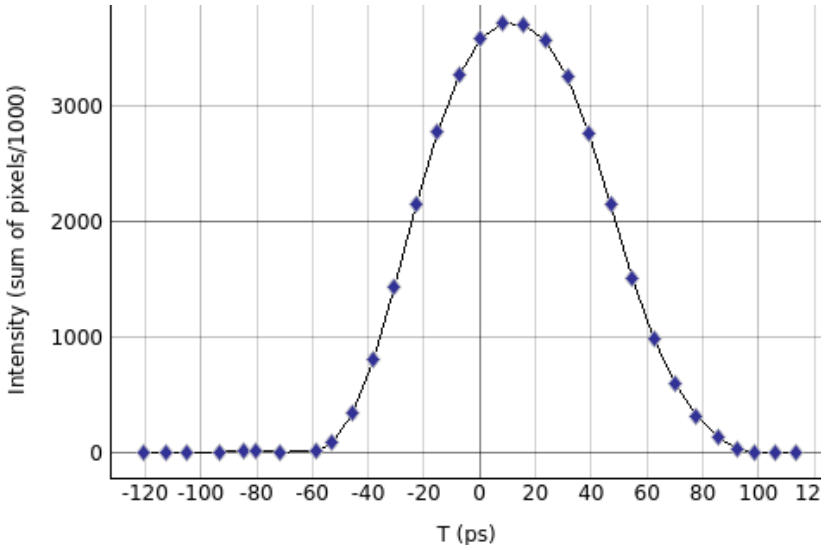


Figure 4: Longitudinal profile of the LeREC electron beam. The shape is close to gaussian with FWHM equal to 77 ps.

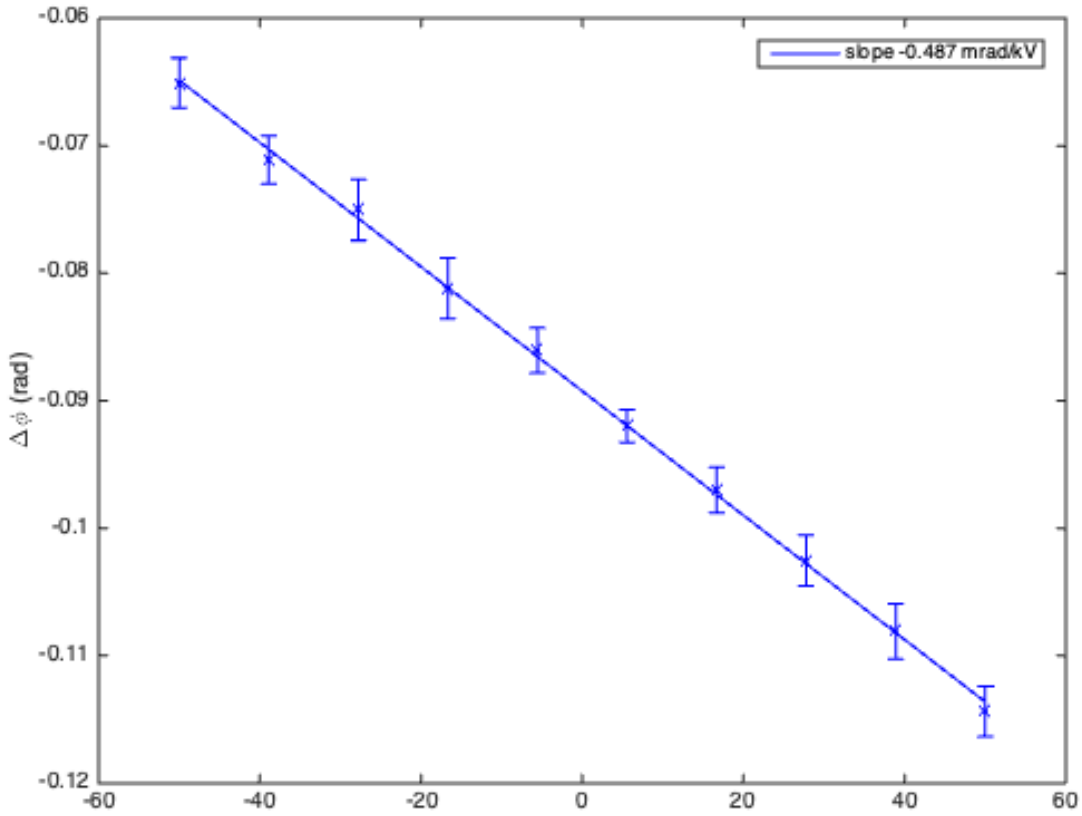


Figure 5: The measurement of the longitudinal tilt with LeREC deflecting cavity. R.m.s. bunch length is 32.7 ps. The phase shift between BPM channels is about 19.5 mrad for 40 kV cavity voltage (estimate is 18.8 mrad).

For CeC beam energy is E_{kin} = 14.05 MeV (γ=28.5). The 1.3 GHz deflecting cavity has 100 kV maximal voltage. BPMs are tuned to 500 MHz ($\omega = \pi \times 10^9$), distance from the cavity to BPM2 is 2.73 m with scaling factor S_2=64.9 m^{-1} (k=15.4 mm), distance from the cavity to BPM3 is 4.64 m with scaling factor S_3=46.7 m^{-1} (k=21.4 mm). Distance from cavity to yag1 is 4.92 m.

The CeC bunch current profile is not gaussian as it is shown in Fig. 7, and we need do develop new equations for calculating the expected phase shift. The amplitude of the induced signal on the button is proportional to the derivative of the longitudinal bunch charge density

$$U(t) \sim \dot{q}(t) = \frac{1}{c}\frac{dI(t)}{dt} \tag{11}$$

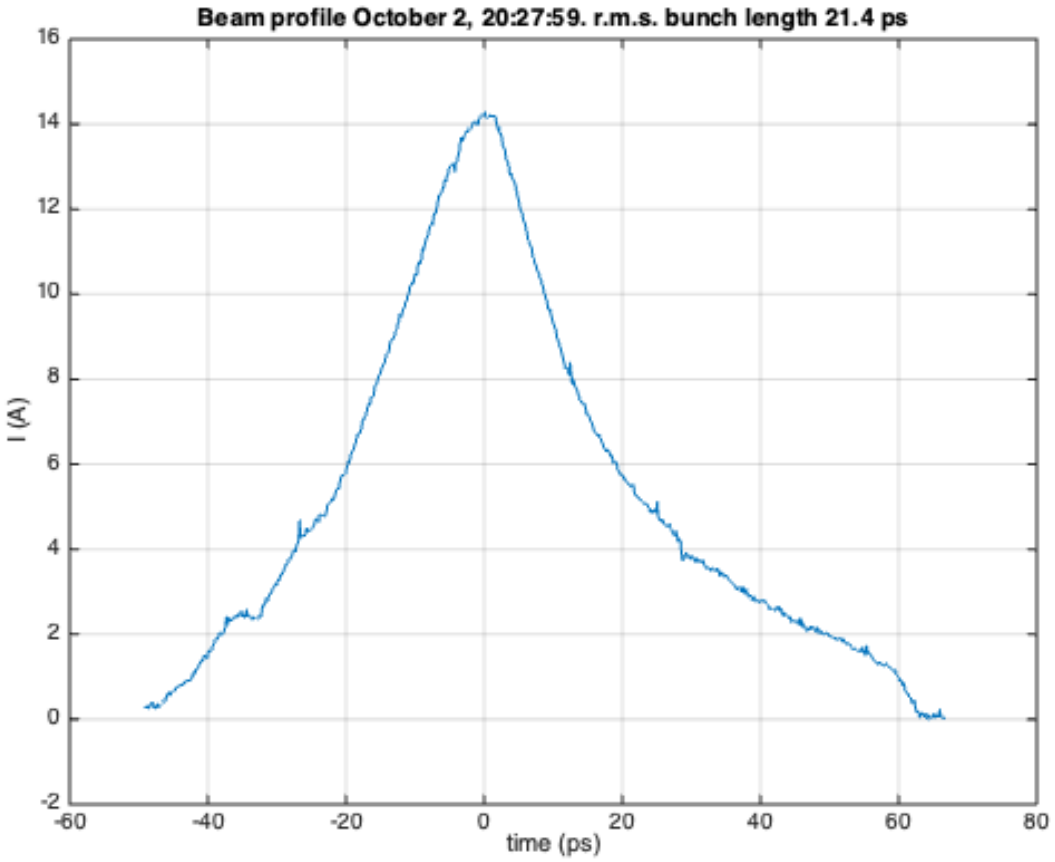


Figure 7: CeC bunch current profile.

We can re-write Eq. 3 as

$$\begin{aligned} U_{cosA,B} &\sim \int_{-\infty}^{8} \frac{dI(t)}{dt}(1 \pm S\alpha ct)\cos\omega_{BPM}t\,dt \\ U_{sinA,B} &\sim \int_{-\infty}^{8} \frac{dI(t)}{dt}(1 \pm S\alpha ct)\sin\omega_{BPM}t\,dt \end{aligned} \tag{12}$$

After integration by parts and taking into the account that current density is zero at infinity

$$U_{cosA,B} \sim -\int_{-\infty}^{8} I(t)\frac{d(1\pm S\alpha ct)\cos\omega_{BPM}t}{dt}dt$$
$$U_{sinA,B} \sim -\int_{-\infty}^{8} I(t)\frac{d(1\pm S\alpha ct)\sin\omega_{BPM}t}{dt}dt \quad (13)$$

or

$$U_{cosA,B} \sim -\int_{-\infty}^{8} I(t)[\pm S\alpha c\cos\omega_{BPM}t - \omega_{BPM}(1\pm S\alpha ct)\sin\omega_{BPM}t]dt$$
$$U_{sinA,B} \sim -\int_{-\infty}^{8} I(t)[\pm S\alpha c\sin\omega_{BPM}t + \omega_{BPM}(1\pm S\alpha ct)\cos\omega_{BPM}t]dt \quad (14)$$

Now, these formulas can be utilized in the script using numerical integration of the current profile data from the screen for calculation of the phase shift. 75 kV voltage of the deflecting cavity provides longitudinal tilt of 0.383 radians for BPM2 and 0.651 radians for BPM3.
For the shown current profile the phase shifts are expected for the BPM2 25.6 mrad and for the BM3 38.8 mrad. The measured phase shifts are 26.5 and 33.5 mrad, respectively.

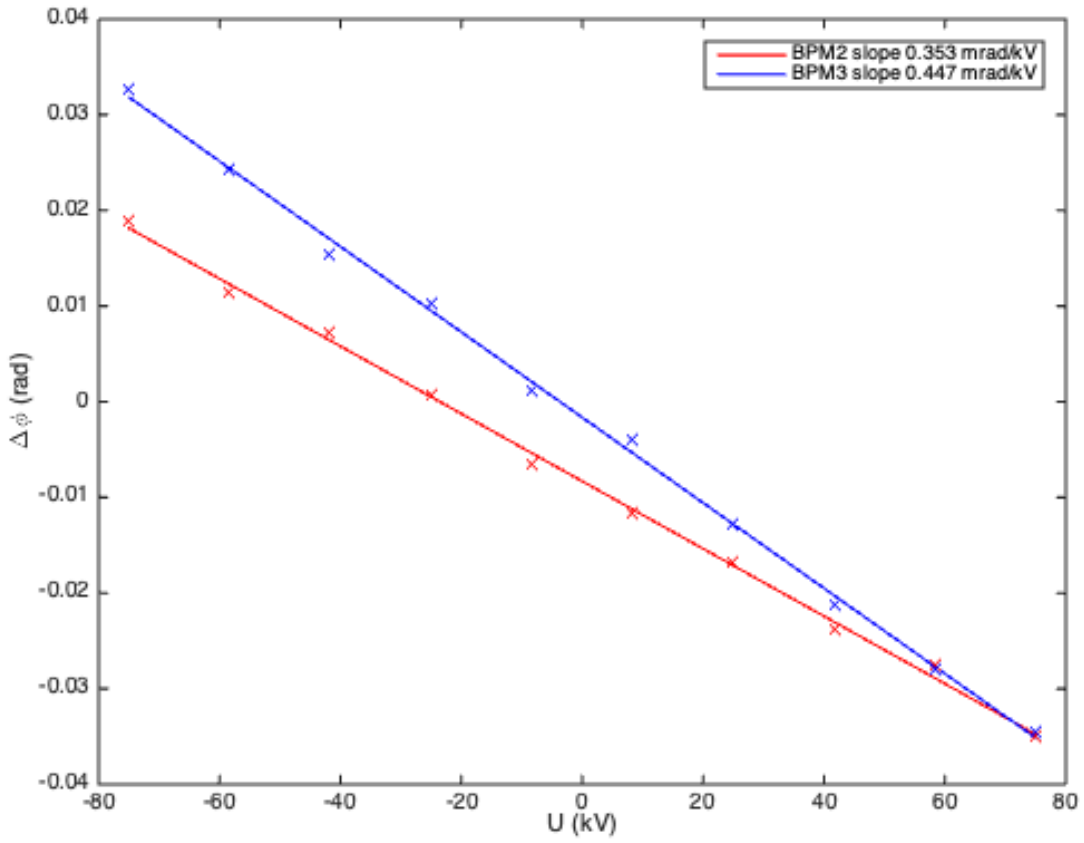


Figure 8: The dependence of the phase shift on the deflecting cavity voltage is shown.

The proposed method can be used for monitoring the crabbing angle using the pick-up electrodes located inside the interaction region. Pick-up electrodes outside the interaction region can be used for monitoring the crab angle closure as well as for feedback on the crab cavity RF system for preventing emittance growth [12, 13].

References

[1] F. Willeke et al., "Electron-Ion Collider Conceptual Design Report 2021", Technical Report BNL-221006-2021-FORE, https://doi.org/10.2172/1765663

[2] K. Ohmi et al., (KEK), Crab crossing at KEKB, Beam-beam workshop, July 2-4, 2007, SLAC

[3] H.Ikeda, J.Flanagan, H.Fukuma, S. Hiramatsu, and T.Mitsuhashi, Crabbing Angle Measurement by Streak Camera at KEKB, Proc. of PAC'07, Albuquerque, New Mexico, USA

[4] H.Ikeda, J.Flanagan, H.Fukuma, and T.Mitsuhashi, Improved Measurement of Crabbing Angle by a Streak Camera at KEKB, Proc. of IPAC'10, Kyoto, Japan

[5] P. Tenenbaum, J. Frisch, D. McCormick, M. Ross, S. Smith, Beam Tilt Signals as Emittance Diagnostics in the Next Linear Collider Main Linac, Proc. of EPAC'02, Paris, France

[6] M. Ross, J. Frisch, D. McCormick, H. Hayano, RF Cavity BPMs as Beam Angle and Beam Correlation Monitors, Proc. of PAC'03, Portland, OR, USA

[7] X. Sun, G. Decker, N. Sereno, Simulation Studies of Button Pickup Electrode Response to Longitudinally Tilted Beams, Proc. of BIW'12, Newport News, VA, USA

[8] N.S. Sereno, G. Decker, R. Lill, X. Sun, B-X Yang, Impact of Longitudinally Tilted Beams on BPM Performance at the Advance Photon Source, Proc. of BIW'12, Newport News, VA, USA

[9] S.R. Smith, "Beam Position Monitor Engineering", AIP Conf. Proc. 390, 50–65 (1997), https://doi.org/10.1063/1.52306

[10] W. Guo, B. Yang, C.-x. Wang, K. Harkay, and M. Borland, Generating picosecond x-ray pulses in synchrotron light sources using dipole kickers, Phys. Rev. ST Accel. Beams 10, 020701.

[11] https://www.i-tech.si/products/libera-single-pass-e/

[12] P. Baudrenghien, T. Mastoridis, Transverse emittance growth due to RF noise in high-luminosity LHC crab cavities, PHYSICAL REVIEW SPECIAL TOPICS—ACCELERATORS AND BEAMS 18, 101001 (2015).

[13] K. Smith, T. Mastoridis, P. Fuller, P. Mahvi, Y. Matsumura, EIC transverse emittance growth due to crab cavity noise: estimates and mitigation, Technical Report BNL-222748-2022-TECH